The 2D Hubbard model and the pseudogap: a COM(SCBA) study

2007 J. Phys.: Condens. Matter 19 255209

(http://iopscience.iop.org/0953-8984/19/25/255209)

IOP PUBLISHING JOURNAL OF PHYSICS: CONDENSED MATTER

J. Phys.: Condens. Matter **19** (2007) 255209 (15pp) doi:10.1088/0953-8984/19/25/255209

The 2D Hubbard model and the pseudogap: a COM(SCBA) study

Adolfo Avella and Ferdinando Mancini

Dipartimento di Fisica 'E R Caianiello', Unità CNISM di Salerno, Università degli Studi di Salerno, I-84081 Baronissi (SA), Italy

E-mail: avella@sa.infn.it

Received 23 September 2006
Published 30 May 2007
Online at stacks.iop.org/JPhysCM/19/255209

Abstract

The two-dimensional Hubbard model is studied within the composite operator method (COM) with the electronic self-energy computed in the self-consistent Born approximation (SCBA). The main idea of the COM is to describe interacting electrons in terms of the composite elementary excitations appearing in the system owing to strong correlations; the residual interactions among these excitations are treated within the SCBA. By analysing the spectral function $A(\mathbf{k}, \omega)$ on varying the filling, we find, at high doping, the ordinary Fermi-liquid behaviour of a weakly interacting metal and, at low doping, the opening of a pseudogap, as reported for cuprates superconductors.

1. Introduction

One of the most intriguing challenges in modern condensed matter physics is the theoretical description of the anomalous behaviours experimentally observed in novel materials. By anomalous behaviours we mean those not predicted by standard many-body theory; that is, behaviours in contradiction with Fermi-liquid framework and diagrammatic expansions. The most important characteristic of novel materials is the strong correlation among electrons that makes inapplicable classical schemes based on the band picture. It is necessary to pass from a *single-electron* physics to a *many-electron* physics, where the dominant contribution comes from the correlations among the electrons. Usual perturbation schemes are inadequate and new concepts must be introduced.

The *classical* techniques are based on the hypothesis that the interaction among the electrons is weak and can be treated in the framework of perturbation schemes. However, as many experimental and theoretical studies of highly correlated electron systems have shown with more and more convincing evidence, all these methods are no more adequate and different approaches must be considered. The main concept that breaks down is the existence of the electrons as particles with some well-defined and intrinsic properties. The presence of interaction modifies the properties of the particles and at a macroscopic level, the

level of observation, what are observed are new particles with new peculiar properties entirely determined by the dynamics and by the boundary conditions. These new objects appear as the final result of the modifications imposed by the interactions on the original particles and contain, at the very beginning, the effects of correlations.

On the basis of this evidence, one can be induced to move attention from the original fields to the new fields generated by the interaction. The operators describing these excitations, once they have been found, can be written in terms of the original ones and are known as composite operators.

The necessity of developing a formulation to treat composite excitations as fundamental objects has been noticed for the many-body problem of condensed matter physics long ago. Recent years have seen remarkable developments in many-body theory in the form of an assortment of techniques that may be termed composite particle methods. The beginnings of these types of techniques may be traced back to the work of Bogoliubov [1] and later to that of Dancoff [2]. The work of Zwanzig [3], Mori [4] and Umezawa [5] has to be mentioned. Closely related to this work is that of Hubbard [6–8], Rowe [9], Roth [10] and Tserkovnikov [11, 12]. The slave boson method [13–15], the spectral density approach [16, 17] and the composite operator method (COM) [18] are also along similar lines. This large class of theories is founded on the conviction that an analysis in terms of elementary fields might be inadequate for a system dominated by strong interactions.

All these approaches are very promising because all the different approximation schemes are constructed on the basis of interacting particles: some amount of the interaction is already present in the chosen basis and permits us to overcome the problem of finding an appropriate expansion parameter. However, one price must be paid. In general, the composite fields are neither Fermi nor Bose operators, since they do not satisfy canonical (anti)commutation relations, and their properties, because of the inherent definition, must be self-consistently determined. They can only be recognized as fermionic or bosonic operators according to the number of constituting original particles. New techniques of calculus have to be developed in order to treat with composite fields. In developing perturbation calculations where the building blocks are now the propagators of composite fields, one cannot use the consolidated scheme: diagrammatic expansions, Wick's theorem and many other techniques are no more valid. The formulation of the Green's function (GF) method must be revisited and new frameworks of calculations have to be formulated.

Following these ideas, in the last few years we have been developing a systematic approach (COM) to the study of highly correlated systems. The formalism is based on two main ideas: (i) propagators of composite operators as building blocks at the basis of approximate calculations; (ii) use of algebra constraints to fix the representation of the GF in order to maintain the algebraic and symmetry properties; these constraints will determine the unknown parameters appearing in the formulation due to the non-canonical algebra of composite operators.

Cuprate superconductors, which are turning 20 years old this year [19], display a full range of anomalous features, mainly appearing in the underdoped region, in almost all experimentally measurable physical properties [20–22]. According to this, their microscopic description is still an open problem: non-Fermi-liquid response, quantum criticality, pseudogap formation, ill-defined Fermi surface, kinks in the electronic dispersion, etc remain still unexplained (or at least controversially debated) anomalous features [23, 24]. Unfortunately, although fundamental for benchmarking and fine-tuning analytical theories, numerical approaches [25] cannot be of help to solve the puzzle of underdoped cuprates owing to their limited resolution in frequency and momentum. On the other hand, there are not so many analytical approaches capable of dealing with the quite complex aspects of underdoped cuprates phenomenology. Among others, the most promising approaches available in the literature can be divided into two classes. One class

makes use of phenomenological expressions for the electronic self-energy and the electronic spin susceptibility [26–28]. The electronic self-energy is usually computed as the convolution of the electronic propagator and of the electronic spin susceptibility. Then, the electronic spin susceptibility is modelled phenomenologically, parameterizing correlation length and damping as functions of doping and temperature according to the common belief that the electronic spin susceptibility should present a well-developed mode at $M = (\pi, \pi)$ with a damping of Landau type. All cluster-dynamical-mean-field-like theories (the cellular dynamical mean-field theory [29], the dynamical cluster approximation [30] and the cluster perturbation theory [31]) belong to the second class. These theories usually self-consistently map the generic Hubbard problem to a few-site lattice Anderson problem and solve this latter by means of, mainly, numerical techniques. What really distinguishes one formulation from another, within this second class, is the procedure used to map the small cluster on the infinite lattice. Anyway, it is worth noticing that these approaches often rely on numerical methods (with the above-mentioned limitations in frequency and momentum resolutions) in order to close their self-consistency cycles. The COM(SCBA) does not belong to any of these two classes of theoretical formulations as it is completely microscopic, exclusively analytical, and fully self-consistent. Starting from a basis of n composite operators (the two Hubbard operators in this specific case), the Dyson equation is formulated in terms of the n-pole approximated Green's function instead of the electronic non-interacting Green's function. According to this, the residual self-energy is the propagator of higher-order composite operators (higher order with respect to the composite operators belonging to the chosen basis). In particular, in the case analysed in the manuscript, the residual self-energy is the propagator of the electronic operators dressed by charge, spin, and pair fluctuations on the nearest-neighbour sites. Then, within the SCBA, we have shown that it is possible to *microscopically* obtain a residual self-energy written in terms of the convolution of the electronic propagator and of the electronic charge, spin, and pair susceptibilities. Finally, we compute the susceptibilities within a pole approximation and close, fully analytically, the self-consistency cycle.

In this manuscript, we will show how it is possible to get some of the experimentally observed underdoped cuprate behaviours in the two-dimensional Hubbard model within a completely analytical self-consistent approach, the composite operator method (COM) [18] with electronic self-energy computed in the self-consistent Born approximation (SCBA) [32]. We will show how Fermi arcs develop out of a large Fermi surface and how pseudogap shows itself in the dispersion.

2. The two-dimensional Hubbard model

The Hamiltonian of the two-dimensional Hubbard model reads as

$$H = \sum_{\mathbf{ij}} (-\mu\delta_{\mathbf{ij}} - 4t\alpha_{\mathbf{ij}}) c^{\dagger}(i)c(j) + U \sum_{\mathbf{i}} n_{\uparrow}(i)n_{\downarrow}(i) \tag{1}$$

where

$$c(i) = \begin{pmatrix} c_{\uparrow}(i) \\ c_{\downarrow}(i) \end{pmatrix} \tag{2}$$

is the electron field operator in spinorial notation and the Heisenberg picture ($i = (\mathbf{i}, t_i)$), $\mathbf{i} = \mathbf{R_i}$ is a vector of the Bravais lattice, $n_{\sigma}(i) = c^{\dagger}_{\sigma}(i)c_{\sigma}(i)$ is the particle density operator for spin σ, $n(i) = \sum_{\sigma} n_{\sigma}(i)$ is the total particle density operator, μ is the chemical potential, t is the hopping integral, and the energy unit, U, is the Coulomb on-site repulsion and $\alpha_{\mathbf{ij}}$ is the

projector on the nearest-neighbour sites

$$\alpha_{\mathbf{ij}} = \frac{1}{N}\sum_{\mathbf{k}} \mathrm{e}^{\mathrm{i}\mathbf{k}\cdot(\mathbf{R_i}-\mathbf{R_j})}\alpha(\mathbf{k}) \qquad \alpha(\mathbf{k}) = \tfrac{1}{2}[\cos(k_x a) + \cos(k_y a)] \tag{3}$$

where $\mathbf{k}$ runs over the first Brillouin zone, N is the number of sites and a is the lattice constant.

2.1. Green's function and Dyson equation for composite fields

Following COM prescriptions [18], we chose a basic field; in particular, we select the composite doublet field operator

$$\psi(i) = \begin{pmatrix} \xi(i) \\ \eta(i) \end{pmatrix} \tag{4}$$

where $\eta(i) = n(i)c(i)$ and $\xi(i) = c(i) - \eta(i)$ are the Hubbard operators describing the main subbands. This choice is guided by the hierarchy of the equations of motion and by the fact that $\xi(i)$ and $\eta(i)$ are eigenoperators of the interacting term in the Hamiltonian (1). The field $\psi(i)$ satisfies the Heisenberg equation

$$\mathrm{i}\frac{\partial}{\partial t}\psi(i) = J(i) = \begin{pmatrix} -\mu\xi(i) - 4tc^{\alpha}(i) - 4t\pi(i) \\ (U-\mu)\eta(i) + 4t\pi(i) \end{pmatrix} \tag{5}$$

where the higher-order composite field $\pi(i)$ is defined by

$$\pi(i) = \tfrac{1}{2}\sigma^{\mu}n_{\mu}(i)c^{\alpha}(i) + c(i)c^{\dagger\alpha}(i)c(i) \tag{6}$$

with the following notation: $n_{\mu}(i) = c^{\dagger}(i)\sigma_{\mu}c(i)$ is the particle- ($\mu = 0$) and spin- ($\mu = 1, 2, 3$) density operator, and $\sigma_{\mu} = (1, \vec{\sigma})$, $\sigma^{\mu} = (-1, \vec{\sigma})$, σ_k ($k = 1, 2, 3$) are the Pauli matrices. Hereafter, for any operator $\Phi(i)$, we use the notation $\Phi^{\alpha}(\mathbf{i}, t) = \sum_{\mathbf{j}} \alpha_{\mathbf{ij}}\Phi(\mathbf{j}, t)$.

It is always possible to decompose the source $J(i)$ under the form

$$J(i) = \varepsilon(-\mathrm{i}\nabla)\psi(i) + \delta J(i) \tag{7}$$

where the linear term represents the projection of the source on the basis $\psi(i)$ and is calculated by means of the equation

$$\langle\{\delta J(\mathbf{i}, t),\ \psi^{\dagger}(\mathbf{j}, t)\}\rangle = 0 \tag{8}$$

where $\langle\cdots\rangle$ stands for the thermal average taken in the grand-canonical ensemble.

This constraint assures that the residual current $\delta J(i)$ contains all and only the physics orthogonal to the chosen basis $\psi(i)$. The action of the derivative operator $\varepsilon(-\mathrm{i}\nabla)$ on $\psi(i)$ is defined in momentum space

$$\varepsilon(-\mathrm{i}\nabla)\psi(i) = \varepsilon(-\mathrm{i}\nabla)\frac{1}{\sqrt{N}}\sum_{\mathbf{k}} \mathrm{e}^{\mathrm{i}\mathbf{k}\cdot\mathbf{R_i}}\psi(\mathbf{k}, t) = \frac{1}{\sqrt{N}}\sum_{\mathbf{k}} \mathrm{e}^{\mathrm{i}\mathbf{k}\cdot\mathbf{R_i}}\varepsilon(\mathbf{k})\psi(\mathbf{k}, t) \tag{9}$$

where $\varepsilon(\mathbf{k})$ is named the energy matrix.

The constraint (8) gives

$$m(\mathbf{k}) = \varepsilon(\mathbf{k})I(\mathbf{k}) \tag{10}$$

after defining the normalization matrix

$$I(\mathbf{i}, \mathbf{j}) = \langle\{\psi(\mathbf{i}, t),\ \psi^{\dagger}(\mathbf{j}, t)\}\rangle = \frac{1}{N}\sum_{\mathbf{k}} \mathrm{e}^{\mathrm{i}\mathbf{k}\cdot(\mathbf{R_i}-\mathbf{R_j})}I(\mathbf{k}) \tag{11}$$

and the m-matrix

$$m(\mathbf{i}, \mathbf{j}) = \langle\{J(\mathbf{i}, t),\ \psi^{\dagger}(\mathbf{j}, t)\}\rangle = \frac{1}{N}\sum_{\mathbf{k}} \mathrm{e}^{\mathrm{i}\mathbf{k}\cdot(\mathbf{R_i}-\mathbf{R_j})}m(\mathbf{k}). \tag{12}$$

Since the components of $\psi(i)$ contain composite operators, the normalization matrix $I(\mathbf{k})$ is not the identity matrix and defines the spectral content of the excitations. In fact, the composite operator method has the advantage of describing crossover phenomena as the phenomena in which the weight of some operator is shifted to another one.

By considering the two-time thermodynamic Green's functions [33–35], let us define the retarded function

$$G(i,\, j) = \langle R[\psi(i)\psi^{\dagger}(j)]\rangle = \theta(t_i - t_j)\langle\{\psi(i),\ \psi^{\dagger}(j)\}\rangle. \tag{13}$$

By means of the Heisenberg equation (5) and using the decomposition (7), the Green's function $G(i,\, j)$ satisfies the equation

$$\Lambda(\partial_i)G(i,\, j)\Lambda^{\dagger}(\overleftarrow{\partial_j}) = \Lambda(\partial_i)G_0(i,\, j)\Lambda^{\dagger}(\overleftarrow{\partial_j}) + \langle R[\delta J(i)\delta J^{\dagger}(j)]\rangle \tag{14}$$

where the derivative operator $\Lambda(\partial_i)$ is defined as

$$\Lambda(\partial_i) = \mathrm{i}\frac{\partial}{\partial t_i} - \varepsilon(-\mathrm{i}\nabla_i) \tag{15}$$

and the propagator $G^0(i,\, j)$ is defined by the equation

$$\Lambda(\partial_i)G^0(i,\, j) = \mathrm{i}\delta(t_i - t_j)I(i,\, j). \tag{16}$$

By introducing the Fourier transform

$$G(i,\, j) = \frac{1}{N}\sum_{\mathbf{k}}\frac{\mathrm{i}}{2\pi}\int \mathrm{d}\omega\, \mathrm{e}^{\mathrm{i}\mathbf{k}\cdot(\mathbf{R_i}-\mathbf{R_j})-\mathrm{i}\omega(t_i-t_j)}G(\mathbf{k},\, \omega) \tag{17}$$

equation (14) in momentum space can be written as

$$G(\mathbf{k},\, \omega) = G^0(\mathbf{k},\, \omega) + G^0(\mathbf{k},\, \omega)I^{-1}(\mathbf{k})\Sigma(\mathbf{k},\, \omega)G(\mathbf{k},\, \omega) \tag{18}$$

and can be formally solved as

$$G(\mathbf{k},\, \omega) = \frac{1}{\omega - \varepsilon(\mathbf{k}) - \Sigma(\mathbf{k},\, \omega)}I(\mathbf{k}) \tag{19}$$

where the self-energy $\Sigma(\mathbf{k},\, \omega)$ has the expression

$$\Sigma(\mathbf{k},\, \omega) = B_{\mathrm{irr}}(\mathbf{k},\, \omega)I^{-1}(\mathbf{k}) \tag{20}$$

with

$$B(\mathbf{k},\, \omega) = \mathcal{F}\langle R[\delta J(i)\delta J^{\dagger}(j)]\rangle. \tag{21}$$

The notation $\mathcal{F}$ denotes the Fourier transform and the subscript irr indicates that the irreducible part of the propagator $B(\mathbf{k},\, \omega)$ is taken. Equation (18) is nothing else than the Dyson equation for composite fields and represents the starting point for a perturbative calculation in terms of the propagator $G^0(\mathbf{k},\, \omega)$. This quantity will be calculated in the next section. Then, attention will be given to the calculation of the self-energy $\Sigma(\mathbf{k},\, \omega)$. It should be noted that the computation of the two quantities $G^0(\mathbf{k},\, \omega)$ and $\Sigma(\mathbf{k},\, \omega)$ are intimately related. The total weight of the self-energy corrections is bounded by the weight of the residual source operator $\delta J(i)$. According to this, it can be made smaller and smaller by increasing the components of the basis $\psi(i)$ (e.g. by including higher-order composite operators appearing in $\delta J(i)$). The result of such a procedure will be the inclusion in the energy matrix of part of the self-energy as an expansion in terms of coupling constants multiplied by the weights of the newly included basis operators. In general, the enlargement of the basis leads to a new self-energy with a smaller total weight. However, it is necessary to point out that this process can be quite cumbersome and the inclusion of fully momentum-and frequency-dependent self-energy corrections can be necessary to effectively take into account low-energy and virtual processes. According to this, one can choose a reasonable number of components for the basic set and then use another approximation method to evaluate the residual dynamical corrections.

2.2. Calculation of $G^0(\mathbf{k}, \omega)$

According to equation (16), the free propagator $G^0(\mathbf{k}, \omega)$ is determined by the following expression

$$G^0(\mathbf{k}, \omega) = \frac{1}{\omega - \varepsilon(\mathbf{k})} I(\mathbf{k}). \tag{22}$$

For a paramagnetic state, straightforward calculations give the following expressions for the normalization $I(\mathbf{k})$ and energy $\varepsilon(\mathbf{k})$ matrices:

$$I(\mathbf{k}) = \begin{pmatrix} 1 - n/2 & 0 \\ 0 & n/2 \end{pmatrix} = \begin{pmatrix} I_{11} & 0 \\ 0 & I_{22} \end{pmatrix} \tag{23}$$

$$\begin{aligned} \varepsilon_{11}(\mathbf{k}) &= -\mu - 4tI_{11}^{-1}[\Delta + (1 - n + p)\alpha(\mathbf{k})] \\ \varepsilon_{12}(\mathbf{k}) &= 4tI_{22}^{-1}[\Delta + (p - I_{22})\alpha(\mathbf{k})] \\ \varepsilon_{21}(\mathbf{k}) &= 4tI_{11}^{-1}[\Delta + (p - I_{22})\alpha(\mathbf{k})] \\ \varepsilon_{22}(\mathbf{k}) &= U - \mu - 4tI_{22}^{-1}[\Delta + p\alpha(\mathbf{k})] \end{aligned} \tag{24}$$

where $n = \langle n(i) \rangle$ is the filling and

$$\begin{aligned} \Delta &= \langle \xi^{\alpha}(i)\xi^{\dagger}(i) \rangle - \langle \eta^{\alpha}(i)\eta^{\dagger}(i) \rangle \\ p &= \langle n_{\mu}^{\alpha}(i)n_{\mu}(i) \rangle - \langle [c_{\uparrow}(i)c_{\downarrow}(i)]^{\alpha} c_{\downarrow}^{\dagger}(i)c_{\uparrow}^{\dagger}(i) \rangle. \end{aligned} \tag{25}$$

Then, (22) can be written in spectral form as

$$G^0(\mathbf{k}, \omega) = \sum_{n=1}^{2} \frac{\sigma^{(n)}(\mathbf{k})}{\omega - E_n(\mathbf{k}) + \mathrm{i}\delta}. \tag{26}$$

The energy spectra $E_n(\mathbf{k})$ and the spectral functions $\sigma^{(n)}(\mathbf{k})$ are given by

$$E_1(\mathbf{k}) = R(\mathbf{k}) + Q(\mathbf{k}) \qquad E_2(\mathbf{k}) = R(\mathbf{k}) - Q(\mathbf{k}) \tag{27}$$

$$\begin{aligned} \sigma_{11}^{(1)}(\mathbf{k}) &= \frac{I_{11}}{2}\left[1 + \frac{g(\mathbf{k})}{2Q(\mathbf{k})}\right] & \sigma_{11}^{(2)}(\mathbf{k}) &= \frac{I_{11}}{2}\left[1 - \frac{g(\mathbf{k})}{2Q(\mathbf{k})}\right] \\ \sigma_{12}^{(1)}(\mathbf{k}) &= \frac{m_{12}(\mathbf{k})}{2Q(\mathbf{k})} & \sigma_{12}^{(2)}(\mathbf{k}) &= -\frac{m_{12}(\mathbf{k})}{2Q(\mathbf{k})} \\ \sigma_{22}^{(1)}(\mathbf{k}) &= \frac{I_{22}}{2}\left[1 - \frac{g(\mathbf{k})}{2Q(\mathbf{k})}\right] & \sigma_{22}^{(2)}(\mathbf{k}) &= \frac{I_{22}}{2}\left[1 + \frac{g(\mathbf{k})}{2Q(\mathbf{k})}\right] \end{aligned} \tag{28}$$

where

$$\begin{aligned} R(\mathbf{k}) &= -\mu - 4t\alpha(\mathbf{k}) + \frac{1}{2}U - \frac{\varepsilon_{12}(\mathbf{k})}{2I_{11}} \\ Q(\mathbf{k}) &= \frac{1}{2}\sqrt{g^2(\mathbf{k}) + \frac{4\varepsilon_{12}^2(\mathbf{k})I_{22}}{I_{11}}} \\ g(\mathbf{k}) &= -U + \frac{1 - n}{I_{11}}\varepsilon_{12}(\mathbf{k}). \end{aligned} \tag{29}$$

The energy matrix $\varepsilon(\mathbf{k})$ contains three parameters: μ, the chemical potential; Δ, the difference between upper and lower intra-subband contributions to kinetic energy; and p, a combination of the nearest-neighbour charge–charge, spin–spin and pair–pair correlation functions. These parameters will be determined in a self-consistent way by means of algebra constraints in terms of the external parameters n, U, and T.

2.3. Calculation of $\Sigma(\mathbf{k}, \omega)$

The calculation of the self-energy $\Sigma(\mathbf{k}, \omega)$ requires the calculation of the higher-order propagator $B(\mathbf{k}, \omega)$ (cf (21)). We shall compute this quantity by using the self-consistent Born approximation (SCBA). By neglecting the pair term $c(i)c^{\dagger\alpha}(i)c(i)$, the source $J(i)$ can be written as

$$J(\mathbf{i}, t) = \sum_{\mathbf{j}} a(\mathbf{i}, \mathbf{j}, t)\psi(\mathbf{j}, t) \tag{30}$$

where

$$\begin{aligned} a_{11}(\mathbf{i}, \mathbf{j}, t) &= -\mu\delta_{\mathbf{ij}} - 4t\alpha_{\mathbf{ij}} - 2t\sigma^{\mu}n_{\mu}(i)\alpha_{\mathbf{ij}} \\ a_{12}(\mathbf{i}, \mathbf{j}, t) &= -4t\alpha_{\mathbf{ij}} - 2t\sigma^{\mu}n_{\mu}(i)\alpha_{\mathbf{ij}} \\ a_{21}(\mathbf{i}, \mathbf{j}, t) &= 2t\sigma^{\mu}n_{\mu}(i)\alpha_{\mathbf{ij}} \\ a_{22}(\mathbf{i}, \mathbf{j}, t) &= (U - \mu)\delta_{\mathbf{ij}} + 2t\sigma^{\mu}n_{\mu}(i)\alpha_{\mathbf{ij}}. \end{aligned} \tag{31}$$

Then, for the calculation of $B_{\mathrm{irr}}(i, j) = \langle R[\delta J(i)\delta J^{\dagger}(j)]\rangle_{\mathrm{irr}}$, we approximate

$$\delta J(\mathbf{i}, t) \approx \sum_{\mathbf{j}} [a(\mathbf{i}, \mathbf{j}, t) - \langle a(\mathbf{i}, \mathbf{j}, t)\rangle]\psi(\mathbf{j}, t). \tag{32}$$

Therefore

$$B_{\mathrm{irr}}(i, j) = 4t^2 F(i, j)(1 - \sigma_1) \tag{33}$$

where we defined

$$F(i, j) = \langle R[\sigma^{\mu}\delta n_{\mu}(i)c^{\alpha}(i)c^{\dagger\alpha}(j)\delta n_{\lambda}(j)\sigma^{\lambda}]\rangle \tag{34}$$

with $\delta n_{\mu}(i) = n_{\mu}(i) - \langle n_{\mu}(i)\rangle$. The self-energy (20) is written as

$$\Sigma(\mathbf{k}, \omega) = 4t^2 F(\mathbf{k}, \omega) \begin{pmatrix} I_{11}^{-2} & -I_{11}^{-1}I_{22}^{-1} \\ -I_{11}^{-1}I_{22}^{-1} & I_{22}^{-2}. \end{pmatrix} \tag{35}$$

In order to calculate the retarded function $F(i, j)$, first we use the spectral theorem to express

$$F(i, j) = \frac{\mathrm{i}}{2\pi} \int_{-\infty}^{+\infty} \mathrm{d}\omega\, \mathrm{e}^{-\mathrm{i}\omega(t_i - t_j)} \frac{1}{2\pi} \int_{-\infty}^{+\infty} \mathrm{d}\omega' \, \frac{1 + \mathrm{e}^{-\beta\omega'}}{\omega - \omega' + \mathrm{i}\varepsilon} C(\mathbf{i} - \mathbf{j}, \omega') \tag{36}$$

where $C(\mathbf{i} - \mathbf{j}, \omega')$ is the correlation function

$$C(i, j) = \langle \sigma^{\mu}\delta n_{\mu}(i)c^{\alpha}(i)c^{\dagger\alpha}(j)\delta n_{\lambda}(j)\sigma^{\lambda}\rangle = \frac{1}{2\pi} \int \mathrm{d}\omega\, \mathrm{e}^{-\mathrm{i}\omega(t_i - t_j)} C(\mathbf{i} - \mathbf{j}, \omega). \tag{37}$$

Next, we use the mode coupling approximation (SCBA) and approximate

$$\langle \sigma^{\mu}\delta n_{\mu}(i)c^{\alpha}(i)c^{\dagger\alpha}(j)\delta n_{\lambda}(j)\sigma^{\lambda}\rangle \approx \langle \delta n_{\mu}(i)\delta n_{\mu}(j)\rangle\langle c^{\alpha}(i)c^{\dagger\alpha}(j)\rangle. \tag{38}$$

By means of this decoupling and using again the spectral theorem, we finally have

$$\begin{aligned} F(\mathbf{k}, \omega) = \frac{1}{\pi} \int_{-\infty}^{+\infty} \mathrm{d}\omega' \, \frac{1}{\omega - \omega' + \mathrm{i}\delta} \frac{a^2}{(2\pi)^3} \int \mathrm{d}^2 p\, \mathrm{d}\Omega\, \alpha^2(p) \\ \times \left[\tanh\frac{\beta\Omega}{2} + \coth\frac{\beta(\omega' - \Omega)}{2}\right] \Im[G_{cc}(\mathbf{p}, \Omega)]\Im[\chi(\mathbf{k} - \mathbf{p}, \omega' - \Omega)] \end{aligned} \tag{39}$$

where $G_{cc}(\mathbf{k}, \omega)$ is the retarded electronic Green's function (cf (13))

$$G_{cc}(\mathbf{k}, \omega) = \sum_{a,b=1}^{2} G_{ab}(\mathbf{k}, \omega) \tag{40}$$

and

$$\chi(\mathbf{k},\omega) = \mathcal{F}\left\langle R\left[\delta n_\mu(i)\delta n_\mu(j)\right]\right\rangle \tag{41}$$

is the total charge and spin dynamical susceptibility. The result (39) shows that the calculation of the self-energy requires the knowledge of the bosonic propagator (41). This problem will be considered in the following section.

2.4. Calculation of the dynamical susceptibility $\chi(\mathbf{k},\omega)$

In this section we shall present a calculation of the charge–charge and spin–spin propagators (41) within the two-pole approximation. This approximation has shown to be capable of catching correctly many important physical features of Hubbard model dynamics (for all details, see [36]).

Let us define the composite bosonic field

$$N^{(\mu)}(i) = \begin{pmatrix} n_\mu(i) \\ \rho_\mu(i) \end{pmatrix} \qquad \begin{aligned} n_\mu(i) &= c^\dagger(i)\sigma_\mu c(i) \\ \rho_\mu(i) &= c^\dagger(i)\sigma_\mu c^\alpha(i) - c^{\dagger\alpha}(i)\sigma_\mu c(i). \end{aligned} \tag{42}$$

This field satisfies the Heisenberg equation

$$\mathrm{i}\frac{\partial}{\partial t}N^{(\mu)}(i) = J^{(\mu)}(i) = \begin{pmatrix} J_1^{(\mu)}(i) \\ J_2^{(\mu)}(i) \end{pmatrix} \qquad \begin{aligned} J_1^{(\mu)}(i) &= -4t\rho_\mu(i) \\ J_2^{(\mu)}(i) &= U\kappa_\mu(i) - 4tl_\mu(i) \end{aligned} \tag{43}$$

where the higher-order composite fields $\kappa_\mu(i)$ and $l_\mu(i)$ are defined as

$$\begin{aligned} \kappa_\mu(i) &= c^\dagger(i)\sigma_\mu\eta^\alpha(i) - \eta^\dagger(i)\sigma_\mu c^\alpha(i) + \eta^{\dagger\alpha}(i)\sigma_\mu c(i) - c^{\dagger\alpha}(i)\sigma_\mu\eta(i) \\ l_\mu(i) &= c^\dagger(i)\sigma_\mu c^{\alpha^2}(i) + c^{\dagger\alpha^2}(i)\sigma_\mu c(i) - 2c^{\dagger\alpha}(i)\sigma_\mu c^\alpha(i) \end{aligned} \tag{44}$$

and we are using the notation

$$c^{\alpha^2}(\mathbf{i},t) = \sum_{\mathbf{j}} \alpha^2_{\mathbf{ij}} c(\mathbf{j},t) = \sum_{\mathbf{jl}} \alpha_{\mathbf{il}}\alpha_{\mathbf{lj}} c(\mathbf{j},t). \tag{45}$$

We linearize the equation of motion (43) for the composite field $N^{(\mu)}(i)$ by writing

$$\mathrm{i}\frac{\partial}{\partial t}N^{(\mu)}(\mathbf{i},t) = \sum_{\mathbf{j}} \varepsilon^{(\mu)}(\mathbf{i},\mathbf{j})N^{(\mu)}(\mathbf{j},t) \tag{46}$$

where the energy matrix is given by

$$m^{(\mu)}(\mathbf{i},\mathbf{j}) = \sum_{\mathbf{l}} \varepsilon^{(\mu)}(\mathbf{i},\mathbf{l})I^{(\mu)}(\mathbf{l},\mathbf{j}) \tag{47}$$

and the normalization matrix $I^{(\mu)}$ and the $m^{(\mu)}$-matrix have the following definitions

$$I^{(\mu)}(\mathbf{i},\mathbf{j}) = \langle [N^{(\mu)}(\mathbf{i},t),\ N^{(\mu)\dagger}(\mathbf{j},t)]\rangle \tag{48}$$

$$m^{(\mu)}(\mathbf{i},\mathbf{j}) = \langle [J^{(\mu)}(\mathbf{i},t),\ N^{(\mu)\dagger}(\mathbf{j},t)]\rangle. \tag{49}$$

As can be easily verified, in the paramagnetic phase the normalization matrix $I^{(\mu)}$ does not depend on the index μ: charge and spin operators have the same weight. The two matrices $I^{(\mu)}$ and $m^{(\mu)}$ have the following form in momentum space:

$$I^{(\mu)}(\mathbf{k}) = \begin{pmatrix} 0 & I_{12}^{(\mu)}(\mathbf{k}) \\ I_{12}^{(\mu)}(\mathbf{k}) & 0 \end{pmatrix} \tag{50}$$

$$m^{(\mu)}(\mathbf{k}) = \begin{pmatrix} m_{11}^{(\mu)}(\mathbf{k}) & 0 \\ 0 & m_{22}^{(\mu)}(\mathbf{k}) \end{pmatrix} \tag{51}$$

where

$$\begin{aligned} I_{12}^{(\mu)}(\mathbf{k}) &= 4[1-\alpha(\mathbf{k})]C_{cc}^{\alpha} \\ m_{11}^{(\mu)}(\mathbf{k}) &= -4tI_{12}^{(\mu)}(\mathbf{k}) \\ m_{22}^{(\mu)}(\mathbf{k}) &= -4tI_{l_\mu\rho_\mu}(\mathbf{k}) + UI_{\kappa_\mu\rho_\mu}(\mathbf{k}). \end{aligned} \tag{52}$$

The parameter C_{cc}^{α} is the electronic correlation function $C_{cc}^{\alpha} = \langle c^{\alpha}(i)c^{\dagger}(i)\rangle$. The quantities $I_{l_\mu\rho_\mu}(\mathbf{k})$ and $I_{\kappa_\mu\rho_\mu}(\mathbf{k})$ are defined as

$$I_{l_\mu\rho_\mu}(\mathbf{k}) = \mathcal{F}\langle[l_\mu(\mathbf{i},t),\ \rho_\mu^{\dagger}(\mathbf{j},t)]\rangle \qquad I_{\kappa_\mu\rho_\mu}(\mathbf{k}) = \mathcal{F}\langle[\kappa_\mu(\mathbf{i},t),\ \rho_\mu^{\dagger}(\mathbf{j},t)]\rangle. \tag{53}$$

Let us define the causal Green's function

$$G^{(\mu)}(i,j) = \langle T[N^{(\mu)}(i)N^{(\mu)\dagger}(j)]\rangle = \frac{\mathrm{i}a^2}{(2\pi)^3}\int \mathrm{d}^2k\,\mathrm{d}\omega\,\mathrm{e}^{\mathrm{i}\mathbf{k}\cdot(\mathbf{R_i}-\mathbf{R_j})-\mathrm{i}\omega(t_i-t_j)}G^{(\mu)}(\mathbf{k},\boldsymbol{\omega}). \tag{54}$$

By means of the equation of motion (46), the Fourier transform of $G^{(\mu)}(i,j)$ satisfies the following equation:

$$[\omega - \varepsilon^{(\mu)}(\mathbf{k})]G^{(\mu)}(\mathbf{k},\omega) = I^{(\mu)}(\mathbf{k}) \tag{55}$$

where the energy matrix has the explicit form

$$\varepsilon^{(\mu)}(\mathbf{k}) = \begin{pmatrix} 0 & \varepsilon_{12}^{(\mu)}(\mathbf{k}) \\ \varepsilon_{21}^{(\mu)}(\mathbf{k}) & 0 \end{pmatrix} \qquad \begin{aligned} \varepsilon_{12}^{(\mu)}(\mathbf{k}) &= -4t \\ \varepsilon_{21}^{(\mu)}(\mathbf{k}) &= m_{22}^{(\mu)}(\mathbf{k})/I_{12}^{(\mu)}(\mathbf{k}). \end{aligned} \tag{56}$$

The solution of (55) is

$$\begin{aligned} G^{(\mu)}(\mathbf{k},\omega) = \Gamma^{(\mu)}(\mathbf{k})&\left[\frac{1}{\omega+\mathrm{i}\delta} - \frac{1}{\omega-\mathrm{i}\delta}\right] + \sum_{n=1}^{2}\sigma^{(n,\mu)}(\mathbf{k}) \\ &\times\left[\frac{1+f_{\mathrm{B}}(\omega)}{\omega-\omega_n^{(\mu)}(\mathbf{k})+\mathrm{i}\delta} - \frac{f_{\mathrm{B}}(\omega)}{\omega-\omega_n^{(\mu)}(\mathbf{k})-\mathrm{i}\delta}\right] \end{aligned} \tag{57}$$

where $\Gamma^{(\mu)}(\mathbf{k})$ is the zero-frequency function (2×2 matrix) [18] and $f_{\mathrm{B}}(\omega) = [\mathrm{e}^{\beta\omega}-1]^{-1}$ is the Bose distribution function. Correspondingly, the correlation function $C^{(\mu)}(\mathbf{k},\omega) = \langle N^{(\mu)}(i)N^{(\mu)\dagger}(j)\rangle$ has the expression

$$C^{(\mu)}(\mathbf{k},\omega) = 2\pi\Gamma^{(\mu)}(\mathbf{k})\delta(\omega) + 2\pi\sum_{n=1}^{2}\delta[\omega-\omega_n^{(\mu)}(\mathbf{k})][1+f_{\mathrm{B}}(\omega)]\sigma^{(n,\mu)}(\mathbf{k}). \tag{58}$$

The energy spectra $\omega_n^{(\mu)}(\mathbf{k})$ are given by

$$\begin{aligned} \omega_n^{(\mu)}(\mathbf{k}) &= (-)^n\omega^{(\mu)}(\mathbf{k}) \\ \omega^{(\mu)}(\mathbf{k}) &= \sqrt{\varepsilon_{12}^{(\mu)}(\mathbf{k})\varepsilon_{21}^{(\mu)}(\mathbf{k})} \end{aligned} \tag{59}$$

and the spectral functions $\sigma^{(n,\mu)}(\mathbf{k})$ have the following expression:

$$\sigma^{(n,\mu)}(\mathbf{k}) = \frac{I_{12}^{(\mu)}(\mathbf{k})}{2}\begin{pmatrix} \frac{\varepsilon_{12}^{(\mu)}(\mathbf{k})}{\omega_n^{(\mu)}(\mathbf{k})} & 1 \\ 1 & \frac{\varepsilon_{21}^{(\mu)}(\mathbf{k})}{\omega_n^{(\mu)}(\mathbf{k})} \end{pmatrix}. \tag{60}$$

Straightforward but lengthy calculations give for the two-dimensional (2D) system the following expressions for the commutators in (53):

$$\begin{aligned} I_{l_\mu\rho_\mu}(\mathbf{k}) = {}& \tfrac{3}{4}[1-\alpha(\mathbf{k})](12C^{\alpha}+C^{\lambda}+6C^{\mu}) - 3[1-\beta(\mathbf{k})](C^{\alpha}+C^{\mu}) \\ & - \tfrac{3}{4}[1-\eta(\mathbf{k})](C^{\alpha}+C^{\lambda}+2C^{\mu}) + \tfrac{1}{4}[1-\lambda(\mathbf{k})]C^{\lambda} + \tfrac{3}{2}[1-\mu(\mathbf{k})]C^{\mu} \end{aligned} \tag{61}$$

$$\begin{aligned} I_{\kappa_\mu\rho_\mu}(\mathbf{k}) = {}& -2[1-\alpha(\mathbf{k})]D + [1-2\alpha(\mathbf{k})](2E^{\beta}+E^{\eta}) + 2\beta(\mathbf{k})E^{\beta} + \eta(\mathbf{k})E^{\eta} \\ & + [1-2\alpha(\mathbf{k})]a_\mu + \tfrac{1}{4}[b_\mu + 2\beta(\mathbf{k})c_\mu + \eta(\mathbf{k})d_\mu] \end{aligned} \tag{62}$$

where $\alpha(\mathbf{k})$, $\beta(\mathbf{k})$, $\eta(\mathbf{k})$, $\mu(\mathbf{k})$, and $\lambda(\mathbf{k})$ are the Fourier transforms of the projectors on the first, second, third, fourth, and fifth nearest-neighbour sites. The parameters appearing in (61) and (62) are defined by

$$\begin{aligned} E &= \langle c(i)\eta^\dagger(i)\rangle & C^\alpha &= \langle c^\alpha(i)c^\dagger(i)\rangle \\ E^\beta &= \langle c^\beta(i)\eta^\dagger(i)\rangle & C^\lambda &= \langle c^\lambda(i)c^\dagger(i)\rangle \\ E^\eta &= \langle c^\beta(i)\eta^\dagger(i)\rangle & C^\mu &= \langle c^\mu(i)c^\dagger(i)\rangle \end{aligned} \tag{63}$$

$$\begin{aligned} a_\mu &= 2\langle c^\dagger(i)\sigma_\mu c^\alpha(i)c^\dagger(i)\sigma_\mu c^\alpha(i)\rangle - \langle c^{\dagger\alpha}(i)\sigma_\mu\sigma^\lambda\sigma_\mu c^\alpha(i)n_\lambda(i)\rangle \\ b_\mu &= 2\langle c^\dagger(i)\sigma_\mu c^\dagger(i)\sigma_\mu[c(i)c(i)]^\alpha\rangle - \langle c^\dagger(i)\sigma_\mu\sigma^\lambda\sigma_\mu c(i)n^\alpha_\lambda(i)\rangle \\ c_\mu &= 2\langle c^\dagger(i)\sigma_\mu c^\dagger(i^\eta)\sigma_\mu c(i^\alpha)c(i^\alpha)\rangle - \langle c^\dagger(i)\sigma_\mu\sigma^\lambda\sigma_\mu c(i^\eta)n_\lambda(i^\alpha)\rangle \\ d_\mu &= 2\langle c^\dagger(i)\sigma_\mu c^\dagger(i^\beta)\sigma_\mu c(i^\alpha)c(i^\alpha)\rangle - \langle c^\dagger(i)\sigma_\mu\sigma^\lambda\sigma_\mu c(i^\beta)n_\lambda(i^\alpha)\rangle \end{aligned} \tag{64}$$

where we used the notation

$$\begin{aligned} i &= (i_x, i_y, t) & i^\beta &= (i_x + a, i_y + a, t) \\ i^\alpha &= (i_x + a, i_y, t) & i^\eta &= (i_x + 2a, i_y, t). \end{aligned} \tag{65}$$

We see that the bosonic Green's function $G^{(\mu)}(i, j) = \langle T[N^{(\mu)}(i)N^{(\mu)\dagger}(j)]\rangle$ depends on the following set of parameters: Fermionic correlators — C^α, C^λ, C^μ, E^β, E^η, D; bosonic correlators — a_μ, b_μ, c_μ, d_μ; zero-frequency matrix — $\Gamma^{(\mu)}(\mathbf{k})$. The fermionic parameters are calculated through the Fermionic correlation function $C(i, j) = \langle\psi(i)\psi^\dagger(j)\rangle$. The bosonic parameters are determined through symmetry requirements. In particular, the requirement that the continuity equation be satisfied and that the susceptibility be a single-value function at $\mathbf{k} = \mathbf{0}$ leads to the following equations:

$$\begin{aligned} b_\mu &= a_\mu + 3D + 2E^\beta + E^\eta - 6\frac{t}{U}(C_\alpha + C_\lambda - 2C_\mu) \\ c_\mu &= a_\mu - D - 2E^\beta + E^\eta + 6\frac{t}{U}(C_\alpha + C_\lambda - 2C_\mu) \\ d_\mu &= a_\mu - D + 2E^\beta - 3E^\eta - 6\frac{t}{U}(C_\alpha + C_\lambda - 2C_\mu). \end{aligned} \tag{66}$$

The remaining parameters a_μ and $\Gamma^{(\mu)}_{11}(\mathbf{k})$ are fixed by means of the Pauli principle

$$\langle n_\mu(i)n_\mu(i)\rangle = \begin{cases} n + 2D & \text{for } \mu = 0 \\ n - 2D & \text{for } \mu = 1, 2, 3 \end{cases} \tag{67}$$

where $D = \langle n_\uparrow(i)n_\downarrow(i)\rangle$ is the double occupancy, and by the ergodic value

$$\Gamma^{(\mu)}_{11}(\mathbf{k}) = \delta_{\mu,0}\frac{(2\pi)^2}{a^2}\delta^{(2)}(\mathbf{k})\langle n\rangle^2. \tag{68}$$

By putting (68) into (58) we obtain

$$\langle\delta n_\mu(i)\delta n_\mu(j)\rangle = \frac{a^2}{2(2\pi)^2}\sum_{n=1}^{2}\int \mathrm{d}^2k\, \mathrm{e}^{\mathrm{i}\mathbf{k}\cdot(\mathbf{R_i}-\mathbf{R_j})-\mathrm{i}\omega_n^{(\mu)}(\mathbf{k})(t_i-t_j)}\left[1 + \coth\frac{\omega_n^{(\mu)}(\mathbf{k})}{2k_\mathrm{B}T}\right]\sigma_{11}^{(n,\mu)}(\mathbf{k}) \tag{69}$$

$$\langle R[\delta n_\mu(i)\delta n_\mu(j)]\rangle = \frac{\mathrm{i}a^2}{(2\pi)^3}\sum_{n=1}^{2}\int \mathrm{d}^2k\,\mathrm{d}\omega\, \mathrm{e}^{\mathrm{i}\mathbf{k}\cdot(\mathbf{R_i}-\mathbf{R_j})-\mathrm{i}\omega(t_i-t_j)}\frac{\sigma_{11}^{(n,\mu)}(\mathbf{k})}{\omega - \omega_n^{(\mu)}(\mathbf{k}) + \mathrm{i}\delta}. \tag{70}$$

2.5. Outline of the calculation of $G(\mathbf{k}, \omega)$

In this section we will give a sketch of the procedure used to calculate the Green's function $G(\mathbf{k}, \omega)$. The starting point is equation (19), where the two matrices $I(\mathbf{k})$ and $\varepsilon(\mathbf{k})$ are

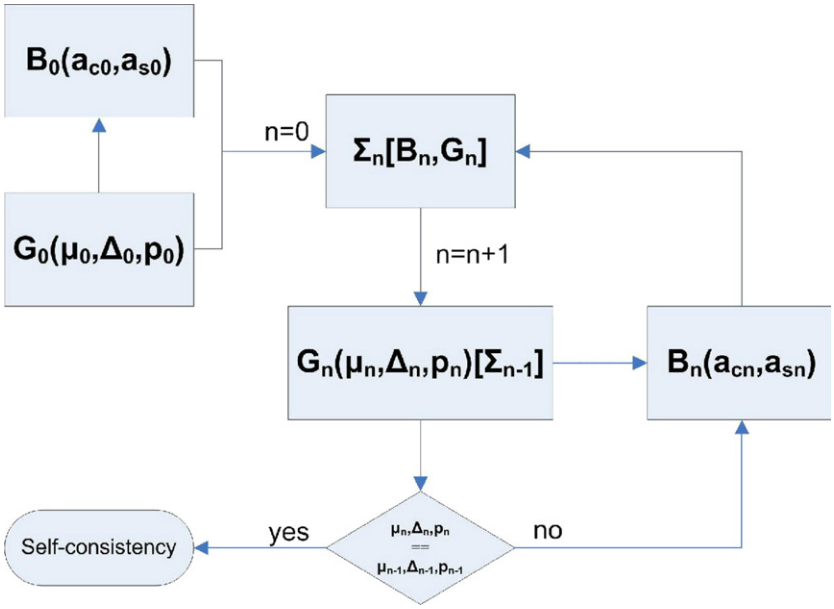

Figure 1. Self-consistency scheme to compute the propagator G in terms of the charge–charge and spin–spin propagator B and the residual self-energy Σ.
(This figure is in colour only in the electronic version)

computed by means of the expressions (23) and (24). The energy matrix $\varepsilon(\mathbf{k})$ depends on three parameters: μ, Δ, and p. To determine these parameters we use the following set of algebra constraints:

$$\begin{aligned} n &= 2(1 - C_{11} - C_{22}) \\ \Delta &= C^{\alpha}_{11} - C^{\alpha}_{22} \\ C_{12} &= \langle \xi(i)\eta^{\dagger}(i)\rangle = 0 \end{aligned} \tag{71}$$

where C and C^{α} are the time-independent correlation functions $C = \langle \psi(i)\psi^{\dagger}(i)\rangle$ and $C^{\alpha} = \langle \psi^{\alpha}(i)\psi^{\dagger}(i)\rangle$. To calculate $\Sigma(\mathbf{k}, \omega)$ we use the SCBA; the results given in section 2.3 show that, within this approximation, $\Sigma(\mathbf{k}, \omega)$ is expressed in terms of the fermionic $G_{cc}(\mathbf{k}, \omega)$ (cf (40)) and of the bosonic $\chi(\mathbf{k}, \omega)$ (cf (41)) propagators. The bosonic propagator is calculated within the two-pole approximation, using the expression (70). As shown in section 2.4, $\chi(\mathbf{k}, \omega)$ depends on both electronic correlation functions (see (63)), straightforwardly computable from $G(\mathbf{k}, \omega)$, and bosonic correlation functions, one per channel, a_c and a_s. The latter are determined by means of the local algebra constraints (67), where n is the filling and D is the double occupancy, determined in terms of the electronic correlation function as $D = n/2 - C_{22}$.

According to this, the electronic Green's function $G(\mathbf{k}, \omega)$ is computed through the self-consistency scheme depicted in figure 1: we first compute $G^0(\mathbf{k}, \omega)$ and $\chi(\mathbf{k}, \omega)$ in two-pole approximation, then $\Sigma(\mathbf{k}, \omega)$ and consequently $G(\mathbf{k}, \omega)$. Finally, we check how much the fermionic parameters (μ, Δ, and p) changed and decide whether to stop or to continue by computing new $\chi(\mathbf{k}, \omega)$ and $\Sigma(\mathbf{k}, \omega)$ after $G(\mathbf{k}, \omega)$. Usually, to get six-digit precision for fermionic parameters, we need eight full cycles to reach self-consistency on a three-dimensional (3D) grid of 128×128 points in momentum space and 4096 Matsubara

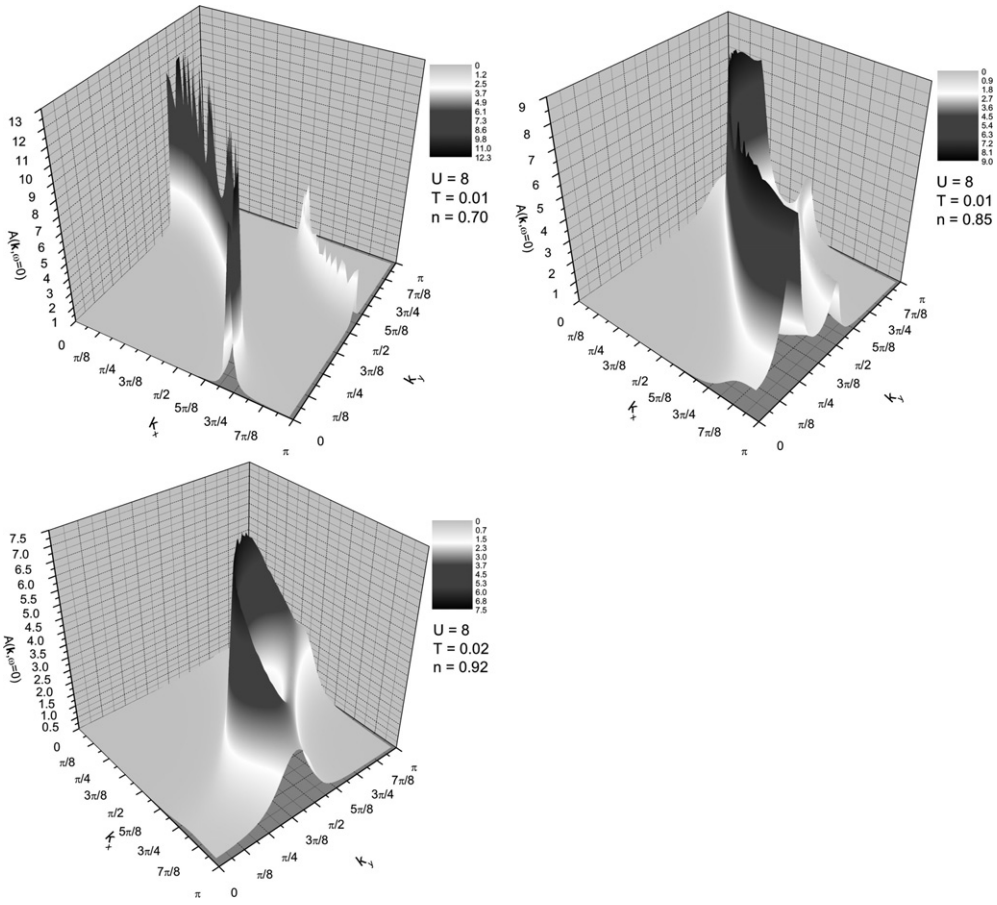

Figure 2. Spectral function at the chemical potential $A(\mathbf{k}, \omega = 0)$ as a function of momentum $\mathbf{k}$ for $U = 8$, (top left) $n = 0.70$ and $T = 0.01$ (top right) $n = 0.85$ and $T = 0.01$ (bottom) $n = 0.92$ and $T = 0.02$.

frequencies. Actually, many more cycles (almost twice as many) are needed at low doping and low temperatures.

Summarizing, within the SCBA and the two-pole approximation for the computation of $\chi(\mathbf{k}, \omega)$, we have constructed an analytical, completely self-consistent scheme of calculation of the electronic propagator $G_{cc}(\mathbf{k}, \omega) = \mathcal{F}\langle T[c(i)c^{\dagger}(j)]\rangle$, where dynamical contributions of the self-energy $\Sigma(\mathbf{k}, \omega)$ are included. All the internal parameters are self-consistently calculated by means of algebra constraints (cf (67), (68) and (71)). No adjustable parameters or phenomenological expressions are introduced. In the next section we shall present some results, by considering the spectral function

$$A(\mathbf{k}, \omega) = -\frac{1}{\pi}\Im[G_{cc}(\mathbf{k}, \omega)]. \tag{72}$$

3. Results

In figure 2, we report the spectral function at the chemical potential $A(\mathbf{k}, \omega = 0) = -\frac{1}{\pi}\Im[G_{cc}(\mathbf{k}, \omega = 0)]$ as a function of momentum k for $U = 8$, $n = 0.70$ and $T = 0.01$

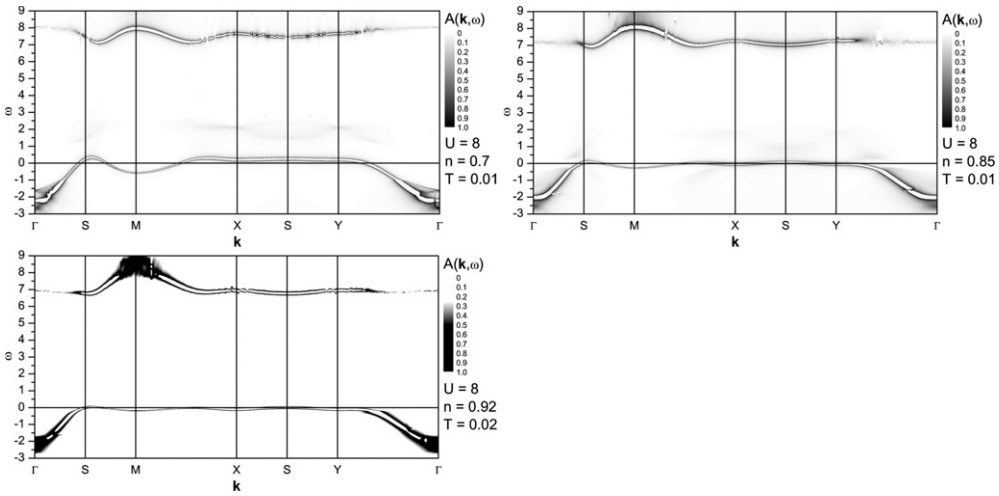

Figure 3. Spectral function $A(\mathbf{k}, \omega)$ along principal directions for $U = 8$, (top left) $n = 0.70$ and $T = 0.01$ (top right) $n = 0.85$ and $T = 0.01$ (bottom) $n = 0.92$ and $T = 0.028$.

(top left panel), $n = 0.85$ and $T = 0.01$ (top right panel) and $n = 0.92$ and $T = 0.02$ (bottom panel). Its maxima mark the effective Fermi surface as measured by ARPES. At large doping ($n = 0.70$), we can recognize the typical behaviour of a weakly interacting Fermi metal: a well-defined Fermi surface. We also have quite a low signal in the proximity of $M = (\pi, \pi)$: the reminiscence of the shadow band (see figure 3). At $n = 0.85$, we report an open Fermi surface: we just passed through the optimal doping ($n \cong 0.82$). This latter is marked by the change in the topology of the Fermi surface between open and close and, consequently, by the coincidence between the value of the chemical potential and the position of the van Hove singularity in the band (see figure 3). At low doping ($n = 0.92$), the situation dramatically changes and the scenario becomes that of a strongly interacting antiferromagnetic metal. The Fermi surface is quite ill defined (it marks an open region of momentum space). The formation of a pseudogap can be immediately deduced by the remarkable difference between the intensities at the cold spots (the well-defined arch departing from $S = (\pi/2, \pi/2)$, the nodal point) and the hot spots (the regions in proximity of $X = (0, \pi)$ and $Y = (\pi, 0)$, the antinodal points). The imaginary part of the self-energy is so intense on the outer part of the hole pocket to reduce it just to an arch as reported by ARPES experiments [21]. The antiferromagnetic fluctuations are so strong as to destroy the coherence of the quasi-particles in that region of momentum space and drive the system towards the transition to a new quantum state.

In figure 3, we report the spectral function $A(\mathbf{k}, \omega)$ along the principal directions ($\Gamma = (0, 0) \rightarrow M$, $M \rightarrow X$, $X \rightarrow Y$ and $Y \rightarrow \Gamma$) for $U = 8$, $n = 0.70$ and $T = 0.01$ (top left panel), $n = 0.85$ and $T = 0.01$ (top right panel) and $n = 0.92$ and $T = 0.02$ (bottom panel). It is worth noticing the extension of the flat region in the dispersion around antinodal points X and Y. It grows systematically on decreasing doping, signalling the transfer of spectral weight from the Fermi surface region as to contrast the destruction of the Fermi surface itself (see figure 2). It is also worth noticing the formation of a hole pocket for the lowest doping. On increasing the filling (reducing the doping), there is an evident transfer of spectral weight between the top of the dispersion band and the antinodal points where van Hove singularities reside.

In conclusion, we have shown how it is possible to obtain a pseudogap scenario in the 2D Hubbard model within the composite operator method with the electronic self-energy

computed in the self-consistent Born approximation. This scenario is just the one that has recently been claimed for underdoped cuprates by ARPES experiments. In particular, we have reported the formation of a pseudogap with related hot and cold spots and arcs on the Fermi surface. It is worth noticing that the proposed formulation is completely microscopic, exclusively analytical, and fully self-consistent. We have clearly shown that bare electrons are just the wrong place to start: composite operators embody the newly formed (because of strong correlations) elementary excitations of the system and constitute the correct starting point for any *perturbation* theory. Dyson equations in terms of composite-operator *non-interacting* propagators immediately show up residual self-energies with the desired mixture of fermionic and bosonic fluctuations. The results that we have found can be summarized as follows: a very low-intensity signal develops around M and moves towards $S = (\pi/2, \pi/2)$ on decreasing doping up to closing, together with the ordinary Fermi surface boundary, a hole pocket in the underdoped regime; whenever a hole pocket develops, it is just the remarkable difference in the intensity of the signal between the two halves of the pocket to make a Fermi arch apparent; the pseudogap develops as a region in momentum (and frequency) with a very low-intensity signal (corresponding to the *phantom* half of the hole pocket) present between the van Hove singularity and the quite *flat* band edge (quite *flat* after the doubling of the Brillouin zone due to the very strong antiferromagnetic fluctuations). We are now planning to include self-energy corrections in the bosonic propagators (in order to analyse, within this framework, the well-known magnetic resonant mode and its hour-glass dispersion) and take into account next- and next-next-nearest-neighbour hopping terms in the Hamiltonian (in order to make quantitative comparisons, and not only qualitative comparisons, with Fermi surface determinations from experiments).

Acknowledgments

We wish to acknowledge gratefully many useful discussions with N M Plakida and P Prelovsek.

References

[1] Bogoliubov N N 1947 *J. Phys. USSR* **11** 23
[2] Dancoff S M 1950 *Phys. Rev.* **78** 382
[3] Zwanzig R 1961 Statistical mechanics of irreversibility *Lectures in Theoretical Physics* vol 3, ed W E Britton, B W Downs and J Downs (New York: Interscience) p 106
[4] Mori H 1965 *Prog. Theor. Phys.* **33** 423
[5] Umezawa H 1993 *Advanced Field Theory: Micro, Macro and Thermal Physics* (New York: AIP) and references therein
[6] Hubbard J 1963 *Proc. R. Soc.* A **276** 238
[7] Hubbard J 1964 *Proc. R. Soc.* A **277** 237
[8] Hubbard J 1964 *Proc. R. Soc.* A **281** 401
[9] Rowe D J 1968 *Rev. Mod. Phys.* **40** 153
[10] Roth L M 1969 *Phys. Rev.* **184** 451
[11] Tserkovnikov Y A 1981 *Teor. Mat. Fiz.* **49** 219
[12] Tserkovnikov Y A 1981 *Teor. Mat. Fiz.* **50** 261
[13] Barnes S E 1976 *J. Phys. F: Met. Phys.* **6** 1375
[14] Coleman P 1984 *Phys. Rev.* B **29** 3035
[15] Kotliar G and Ruckenstein A E 1986 *Phys. Rev. Lett.* **57** 1362
[16] Kalashnikov O K and Fradkin E S 1969 *Sov. Phys.—JETP* **28** 317
[17] Nolting W 1972 *Z. Phys.* **255** 25
[18] Mancini F and Avella A 2004 *Adv. Phys.* **53** 537
[19] Bednorz J G and Müller K A 1986 *Z. Phys.* B **64** 189
[20] Timusk T and Statt B 1999 *Rep. Prog. Phys.* **62** 61

[21] Damascelli A, Hussain Z and Shen Z-X 2003 *Rev. Mod. Phys.* **75** 473
[22] Eschrig M 2006 *Adv. Phys.* **55** 47
[23] Lee P A, Nagaosa N and Wen X-G 2006 *Rev. Mod. Phys.* **78** 17
[24] Tremblay A-M S, Kyung B and Sénéchal D 2006 *Fiz. Nizk. Temp.* **32** 561
[25] Bulut N 2002 *Adv. Phys.* **51** 1587
[26] Chubukov A V and Norman N R 2004 *Phys. Rev.* B **70** 174505 and references therein
[27] Prelovšek P and Ramšak A 2005 *Phys. Rev.* B **72** 012510
[28] Plakida N M and Oudovenko V S 2006 *Preprint* JINR, E-17-2006-96
[29] Kotliar G, Savrasov S Y, Palsson G and Biroli G 2001 *Phys. Rev. Lett.* **87** 186401
[30] Hettler M H, Tahvildar-Zadeh A N, Jarrell M, Pruschke T and Krishnamurthy H R 1998 *Phys. Rev.* B **58** R7475
[31] Sénéchal D, Perez D and Pioro-Ladriére M 2000 *Phys. Rev. Lett.* **84** 522
[32] Bosse J, Götze W and Lücke M 1978 *Phys. Rev.* A **17** 434
[33] Bogoliubov N N and Tyablikov S V 1959 *Dokl. Akad. Nauk. USSR* **126** 53
[34] Zubarev D N 1960 *Sov. Phys.—Usp.* **3** 320
[35] Zubarev D N 1974 *Nonequilibrium Statistical Thermodynamics* (New York: Consultants Bureau)
[36] Avella A, Mancini F and Turkowski V 2003 *Phys. Rev.* B **67** 115123